On the Measurement of Subsonic Flow in a Capacitively Coupled Helicon Plasma Source

2010 J. Phys.: Conf. Ser. 257 012019

(http://iopscience.iop.org/1742-6596/257/1/012019)

25th Summer School and International Symposium on the Physics of Ionized Gases—SPIG 2010 IOP Publishing
Journal of Physics: Conference Series **257** (2010) 012019 doi:10.1088/1742-6596/257/1/012019

On the Measurement of Subsonic Flow in a Capacitively Coupled Helicon Plasma Source

Åshild Fredriksen, Lekha Nath Mishra, Njål Gulbrandsen, and Wojciech J. Miloch
Department of Physics and Technology, Faculty of Science, University of Tromsø, N-9037 Tromsø, Norway

E-mail: ashild.fredriksen@uit.no

Abstract. Plasma parameters and the subsonic flow from a capacitively coupled, cylindrical plasma source of the Njord helicon device are investigated by means of a Mach probe and a retarding field energy analyzer (RFEA). 13.56 MHz and 600 W RF power is inserted into the argon working gas under low-pressure conditions and moderate magnetic field. By means of a downstream field coil, the magnetic field is shaped from a purely expanding field to a configuration with more parallel field lines. It is shown that the downstream plasma density along the outer rim of the source increases significantly and there is a sudden increase by nearly 20 V in the plasma potential already after a moderate increase in the downstream magnetic field. The investigation of the flow indicates that current ratios derived from the Mach probe result in an apparent flow in the direction towards the source, while the current bratios derived from the RFEA indicate a flow in the direction away from the source. PIC simulations demonstrate that the acceptance angle of the probes, being nearly 180^o for the Mach probe, and about 45^o for the RFEA, can critically affect the current ratios and hence the subsonic flow measured by the probes in the weakly magnetized plasma in our device. The first section in your paper

1. Introduction.

It is now well established that the plasma expanding from inductively-coupled helicon source into a larger downstream vacuum chamber, can sustain an electrical double-layer (DL) structure near the entrance to the vacuum chamber [1]. Evidence that this type of DL exists also in the Njord helicon device has been presented earlier [2]. An extensive number of recent studies have not yet found a decisive explanation of the mechanism behind these, so-called current-free DLs, as no external electrical circuit is needed to form them [3-5]. In particular, the role played by the magnetic field in the formation of the DL has been debated. It is well established that it disappears when the field in the source decreases below a certain value [6]. Recent findings show evidence the high density in the source as well as a DL can form also for very low magnetic field [7, 8]. The magnetic field is an important factor in the formation of the DL, but the details of the role it plays are not yet clear. It has been shown that the addition of a downstream magnetic field applied in the expansion chamber, extinguishes the potential drop at the source entrance and subsequently, the DL and the signature beam disappear [9]

In the present paper, we investigate in more detail the measurements of a subsonic flow. We demonstrate how the Mach probe measurements result in reversed flows. The application of the retarding-field energy analyzer (RFEA) probe in the measurement of subsonic flow is investigated and

compared to analysis of simulated data. Finally, the dependence of acceptance angle on the current ratio for Mach number analysis is demonstrated and shown to be in agreement with the actual probe data. In Section 2, we explain the experimental setup and diagnostics. Measurements are reported in Section 3, and the PIC simulations are discussed and compared to our data sets in Section 4.Other paragraphs are indented.

2. Experiment and diagnostics.

The Njord experiment [2] consists of a 0.6m diameter and 1.5m long chamber with a spherical dome at one end. The chamber is pumped to a base pressure of typically 0.05–0.1 mPa. A helicon plasma source with the same specifications as the source of the Chi Kung device at ANU [10] is attached axially on the dome, as shown in Fig. 1. The source is constructed from a 30 cm long Pyrex glass tube with inner diameter 13.8 cm. The outer edge of the tube is chosen as origo of the z-axis for measurements along the centre of the column. A Boswell-type saddle antenna is formed around its outer diameter. The tube and antenna are enclosed by a cylindrical aluminium former, holding a pair of magnetic field coils of diameter 24 cm and width 9.5 cm. The centre of the first coil is placed 18 mm downstream of the outer edge of the Pyrex tube, and the centre of the second is displaced by 20 cm with respect to the centre of the first. Currents of 5 and 7 A in the source coils produce maxima of the magnetic fields of B ≈ 25 mT. At z = 55 cm downstream from origo, a third (guide) coil is placed, close to the intersection between the dome and the main chamber. It produces B ≈ 8 mT at 20A current. 13.56 MHz CW RF power, typically 300–800W forward and less than 50W reflected, is fed from a Henry 8K Ultra amplifier through an air-cooled □-matching network to the antenna Three radially and one axially oriented ports are placed on the dome 50 cm downstream from origo, as indicated in figure 1. Probes can be inserted through these ports for measurements along the axial and radial directions.

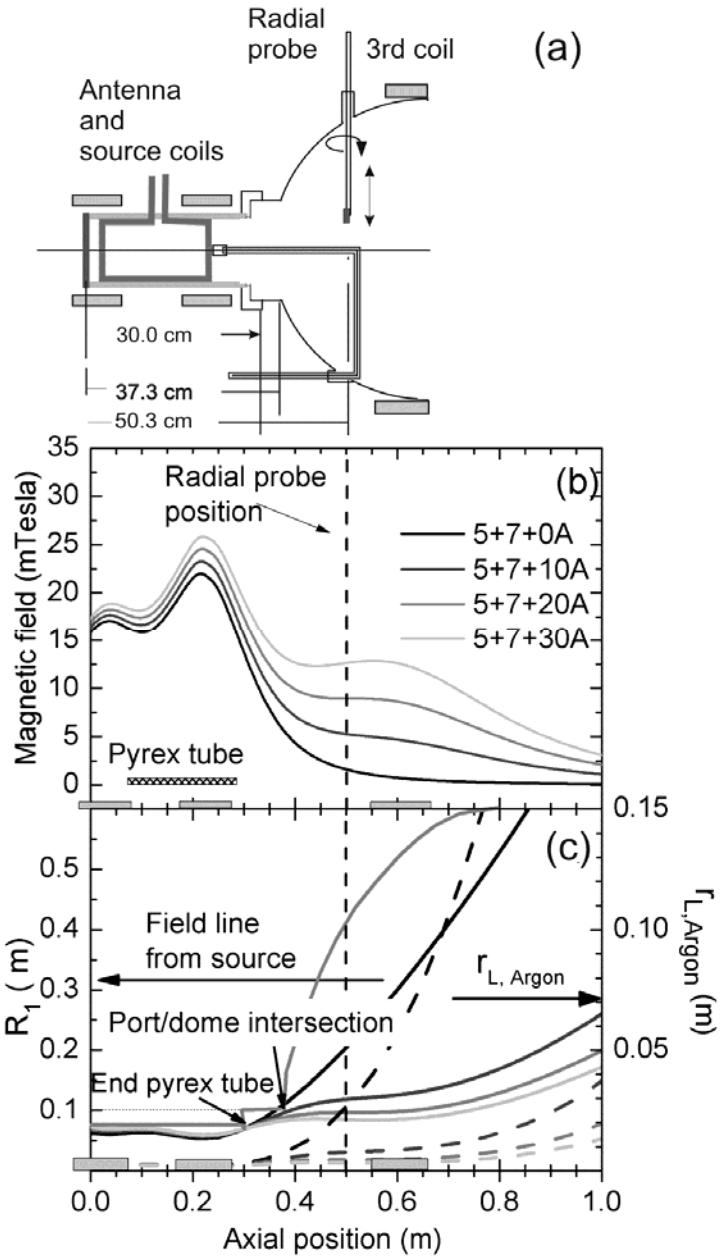

Figure 1. Sketch of the experiment layout (a), axial magnetic field (b), and field line expansion and Larmor radii of ions with axial position (c). Field lines are drawn as full lines with scale at left axis. Dashed lines represent r_L, with scale at right axis.

For the data presented here, a retarding field energy analyzer (RFEA) of outer dimensions WidthxLengthxHeight ≈ 20x40x10 mm was used to obtain plasma potential, beam density and beam

energy. The RFEA placed in the radial port (figure 1) could be rotated 360◦ around its own axis, and background plasma parameters were obtained with the RFEA looking 90◦ to the flow direction. As the plasma is steady state, the total current to the collector could be obtained in both up- and down-stream direction and Mach probe analysis performed (see below). The grids and plates of the RFEAs [11] were organized 0.5mm apart as follows: an aperture plate with a gridded 2mm diameter hole, an electron repeller grid biased at typically −90V, a discriminator grid swept from −100 to +100V at zero offset, a secondary electron repeller grid biased at −18Vand a collector plate at −9V. To capture the energy distribution at the plasma potential, additional batteries between the sweep and the grid produced positive offsets up to 90V in steps of 9V. The discriminator was biased in 400 steps per sweep. At each step, the collector current, measured over a 35.7 kΩ resistor, was digitized into 200 samples which were then averaged into one single value, and stored to the file for further processing. The derivative of the current I(Vd) to the collector as a function of the discriminator bias, is proportional to the ion energy distribution through the relation [11]:

$$f(V_d) = \frac{1}{q} f(E) = \frac{m}{T^4 A q} \frac{1}{v} \frac{dI}{dV_d} \tag{1}$$

where V_d is the bias potential of the discriminator grid, E is the ion energy, q the elementary charge, m the ion mass. T is the transparency of one grid, A the area of the aperture and v is the ion thermal velocity.

Furthermore, a Mach probe, consisting of two parallel 2x4 mm rectangular electrodes separated by ceramic insulation, was used to test direct flow measurements in accordance with standard Mach probe theory [12]. With each electrode biased to -130 V, the ion saturation current I_{sat}^{+} was collected in the upstream direction towards the source (viewing angle $\theta = 0^{o}$) and in the downstream direction looking away from the source ($\theta = 180^{o}$). According to the theory, the Mach number M can be obtained as

$$\frac{I_{sat}^{+}(\theta)}{I_{sat}^{+}(\theta+\pi)} = \frac{\int_{\theta-\Delta\theta}^{\theta+\Delta\theta} j(M,\theta)d\theta}{\int_{\theta-\Delta\theta}^{\theta+\Delta\theta} j(M,\theta+\pi)d\theta} = \exp\left(KM\cos\theta \frac{\sin\Delta\theta}{\Delta\theta} \right) \tag{2}$$

Here, the angle surface normal of the probe, θ, is zero with the probe looking towards the source, and $\Delta\theta$ is the field of view of the probe. I is the total current collected at the probe surface, and j is the current density. K is a constant depending on model and magnetization, with values typically in the range 1.34 to 1.45 [13, 14]. The Mach probe analysis has been most successfully used in magnetized plasmas [13, 15]. Originally proposed for flows in non-magnetized plasma [16], the Mach probe method has been less successful in these plasmas, due to the problem pointed out by Hutchinson [17], and confirmed experimentally by [18]. It was shown that ions from the upstream direction can be deflected and collected at the downstream surface of a Mach probe, resulting in a much lower flow measurement or even a flow reversal. In the experiments presented here, we will show evidence that this effect is important in our plasma, but that ion currents collected by the RFEA are less sensitive to this wake effect.

In the experiments reported here, for the controlled parameters we used RF power of 400–600W, and the argon gas fill pressure was 0.024 Pa (1.5 sccm). The currents in the first and second source coils were set to 5A and 7A, respectively, where the first is at the outer end of the source. The current in the third coil was varied between 0 and 30 A. Some resulting B-fields are shown in figure 1 b).

As the current in the 3rd coil is increased from 0 A to 30 A, the magnetic field at the axial position of the radial ports increases from about 2 mT to about 12 mT, resulting in the argon Larmor radius to decrease from about 5 cm to 5 mm. Within the same B-field range, the radial position of the

field lines emerging from the edge of the source tube decreases from 20 cm to 8 cm at the radial ports, as shown in Fig. 1 c).

It was shown earlier [9] that for lower downstream magnetic fields, these field lines cross the walls of the port supporting the source tube, but as the 3rd coil current increases above about 6-8 A, they are restricted to within the chamber. The confinement of the electrons significantly improves, and the downstream plasma potential increases, eventually destroying the double layer creating the ion beam. From I = 8 A and upwards, a beam can no longer be discerned, and the entire plasma population flows at subsonic speed.

It should be noted that the double layer can be sustained for an inductive tuning of the matching network. In the present investigating of subsonic flows, the antenna was capacitively matched to the RF-power. Thus no beam was generated neither at the lowest downstream magnetic fields.

3. Measurements

Radial profiles of potential and total ion current measured by the RFEA pointed in the normal direction to the flow are shown in Fig. 2. The plot representing density profiles (Fig. 2 a) are obtained from the total areas of Gaussian fits to the derivatives of the 'I vs V'-curves. This method has the advantage that instrumental offsets in the ion current are removed in the derivative. Comparisons with the more commonly used technique of direct reading of the ion saturation current with offsets removed [2, 19], show good agreement, provided a good Gaussian fit to the actual distribution is possible. In the Figure, the capacitive coupling is evident from the hollow density profiles with maxima centred at the field lines arriving from around the edge of the source. The density increases as the magnetic field improves the confinement. The plasma potential profiles, derived from the maximum of the Gaussian fit, have only a small gradient towards the edge of the column. A large increase in potential between 0 and 6 A in the 3rd coil is evident, in agreement with what is found with the RF coupled inductively to the plasma source. For the flow measurements, the RFEA was pointed successively in the up- and down-stream direction to collect the ion energy distribution (IED) in both directions, yielding the total Isat+ by integration of the distribution.

Typical IEDs from two different radial positions at moderate magnetic field of I_3 = 10A, i.e. B = 5 mT and r_L = 1 cm at the probe, are shown in Fig. 3. At the radial position r = 9 cm (Fig. 3 a) the integrated area of the IED at $\theta = 180^o$ is smaller than the area at $\theta = 0^o$, indicating a flow in the positive z-direction away from the source. On the other hand, at r = 4 cm (Fig. 3 b) the integrated area of the IED at $\theta = 180^o$ is slightly larger than that at $\theta = 0^o$, indicating a flow reversal. Also, the Mach probe was used to obtain I_{sat}^+ simultaneously in the up- and downstream direction to deduce flow from the current ratios as given in Eq. 2.

The ratios of the ion saturation currents from the upstream and downstream looking Mach probe are shown in Fig. 4 a) for a set of different downstream magnetic fields, as represented by the 3rd coil current. Apart from the case of the lowest magnetic field which shows a ratio > 1, for all higher magnetic fields, the ratio is less than 1 in most except the outermost of the radial positions, indicating a flow towards the source. The profile is also qualitatively very different from the current ratios obtained by the RFEA, shown in Fig. 4 b). While the current ratios of the RFEA are largest where the largest densities are observed and increasing with density and magnetic field, the Mach probe ratio is decreasing with increasing magnetic field to values down to 0.7. As such values indicate the unphysical situation of a flow towards the source, it is likely that this phenomenon is due to upstream ions being collected by the downstream looking surface of the probe, as demonstrated earlier [17, 18]. On the other hand, the effect is becoming more severe by increasing magnetic field, which is somewhat counter-intuitive, as the Larmor radius is down to about 5 mm (about the size of the Mach probe) at the highest magnetic field. One explanation might be that the plasma potential is increasing rapidly with increasing magnetic field, so that the probe bias with respect to the plasma is increasing, and hence the deflection of the ion trajectories might be stronger.

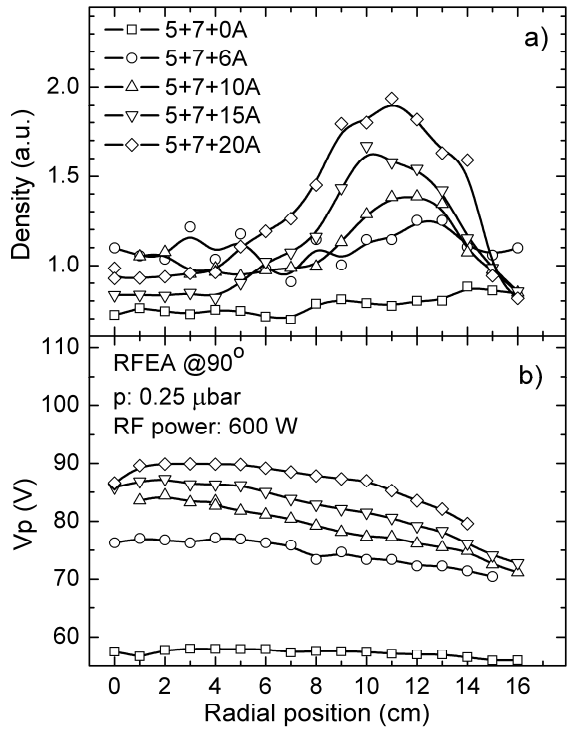

Figure 2. Density profiles (a), and V_p obtained from RFEA looking in the direction normal to the flow, for a set of four different currents in the 3rd coil.

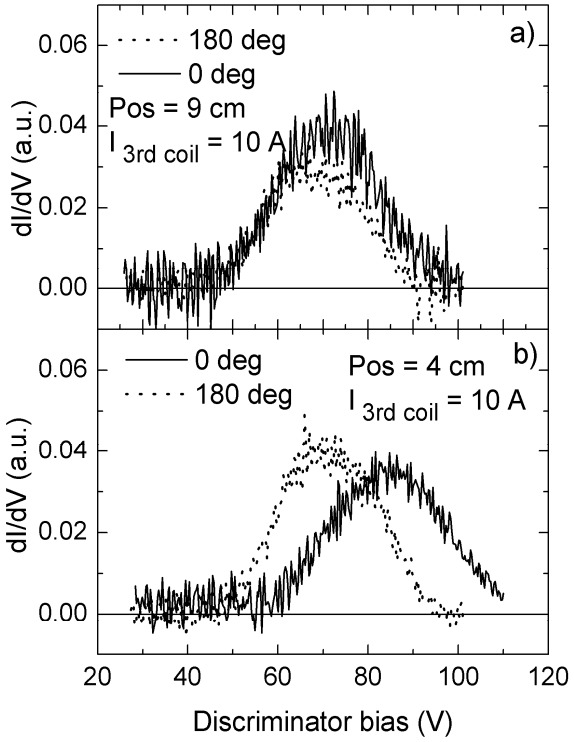

Figure 3 Typical IEDs at a) r = 9 cm and at b) r = 4 cm, with B = 5 mT at the RFEA probe. Full lines are IEDs at $\theta = 0^o$ and dotted lines are IEDs at $\theta = 180^o$

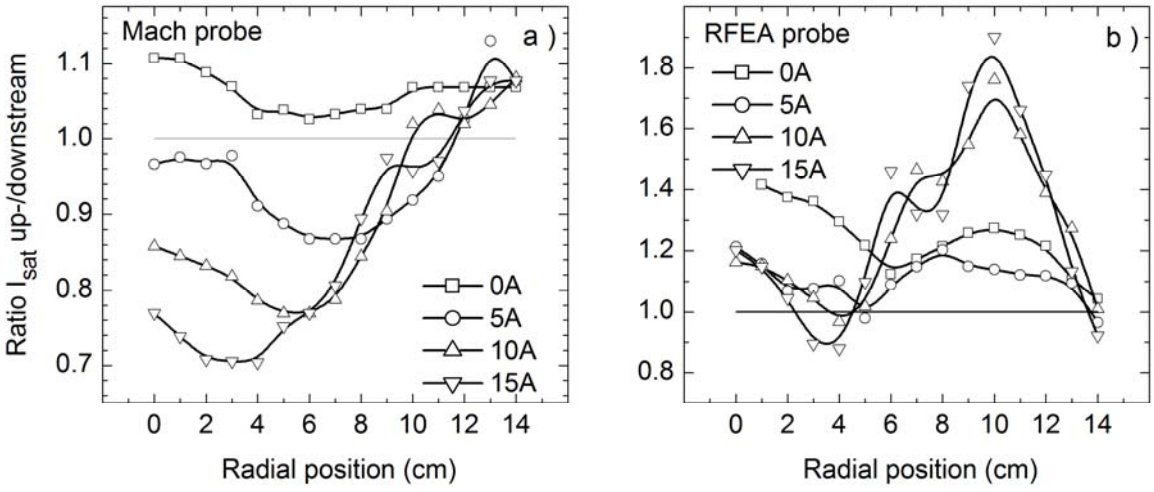

Figure 4 Current ratios from Mach-probe (a), and from up- and down-stream looking RFEA (b)

On the other hand, we also have seen strong indications of an electron beam from the source in Langmuir probe measurements, and this could also represent a possible source of erroneous ion current ratios as well. The ratios of the ion current to the RFEA looking towards the source over the current to the RFEA looking downstream, indicate, quite contrary, flows in the direction away from the source, except from a small region between 3 -4 cm from the axis for 5 A in the 3rd coil. The indicated flow is highly inhomogeneous over the plasma cross-section, which nevertheless is in agreement with the density profile, providing an inhomogeneous plasma pressure which in turn is more confined along the magnetic field as it increases. Thus, it is reasonable that the flow fields are restricted to a more narrow range in the radial positions.

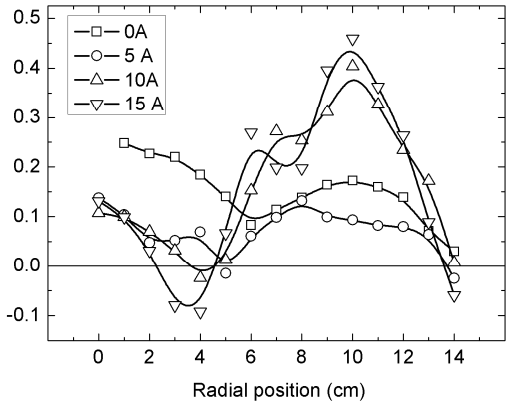

Figure 5. Mach numbers calculated from the current ratios taken form RFEA measurements in Fig. 4 b)

Another point in favour of the RFEA ratios, is the fact that the collecting surfaces of the Mach probe is in direct contact with the plasma, while the probe surface of the RFEA as seen from the plasma, is at ground. This means that the potential difference between the RFEA and the plasma is 130 V less than between the Mach probe and the plasma. Moreover, the RFEA is bigger (2x4 cm), with a smaller collecting aperture of 2 mm. The fact that the aperture at the front creates a total acceptance angle of about 45o prevents the ions with large velocity components parallel to the probe surface from entering. Most of the upstream ions collected at the downstream surface of the Mach probe would have such velocity components, as their trajectories have been bent from a large velocity parallel to the flow. These would be collected by the Mach probe due to its more open-faced geometry, with an acceptance angle of nearly 180 ^{o}. Thus, there are indications that the current ratios measured by the RFEA are more reliable than of the Mach probe for our plasma parameters.

In Fig. 5, the resulting radial profiles Mach numbers obtained from the RFEA data are shown. The value taken for the constant K is taken to be 1.4. The Mach numbers computed from this data set are within comparable range of those measured by others in helicon sources [20]. As the estimated ion acoustic velocity $c_s = (T_e/M_i)^{1/2}$ is 3.5 km/s at an estimated electron temperature T_e of 5 eV and ion mass M_i of argon, the resulting flow speeds would range from about 350 m/s to a maximum of 1500 m/s at the highest magnetic field. To what point it is accurate, is still not yet fully investigated.

4. Simulations

To improve our understanding of flow measurements with the RFEA, we have performed PIC simulations applying the DiP3D code, which has been designed for simulations of objects in complex plasma environments [21, 22], to a set of plasma parameters for some simple cases of subsonic flows, as indicated from the present measurements. For the present study, the code has been upgraded to

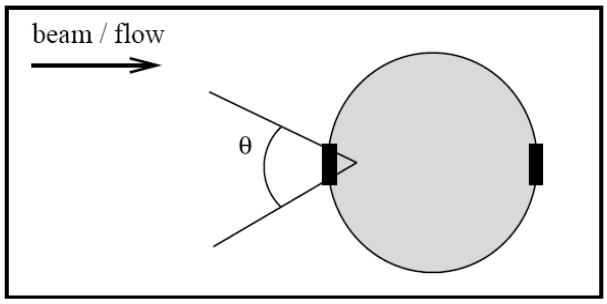

Figure 6. Geometry of the numerical simulations

account also for external uniform magnetic field [23], and collisions [24]. We simulate argon plasma with parameters closely representing typical conditions in the helicon plasma device Njord [9]. The plasma density is n = 2.5 • 10^{16} m^{-3}, and the neutral gas density nn = 2.0 • 10^{19} m^{-3}. The electron and ion temperatures are T_e = 4 eV and T_i = 0.4 eV, respectively. A spherical analyzer of radius $r \approx 4x10^{-4}$ • 10−4 m with the aperture radius a/r = 0.15 and varied acceptance angle θ is placed in the centre of the simulation box of length L = 4 • 10−3 m in each direction, as shown in Fig. 6. The analyzer is biased at Φ = −45 V with respect to the plasma potential. The size of the analyzer is much smaller than in real experiments, which we compensate by a strong magnetic field (B = 0.6 T), ensuring that the ratios of characteristic lengths in the system are maintained. We consider the case of plasma with subsonic flow.

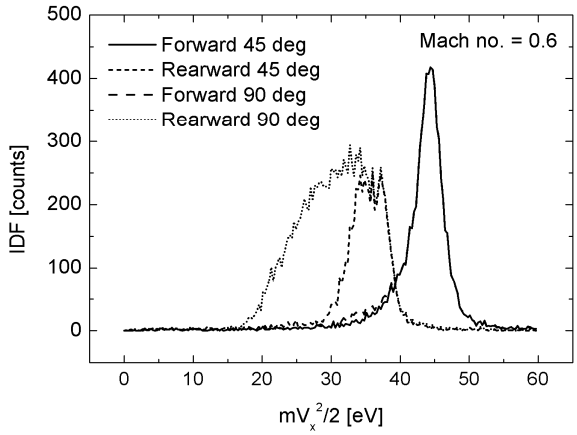

Figure 7. Simulated IEDs, with drift speed 0.6 cs., obtained by a probe with acceptance angles 90° and 45°, in forward and rearward directions.

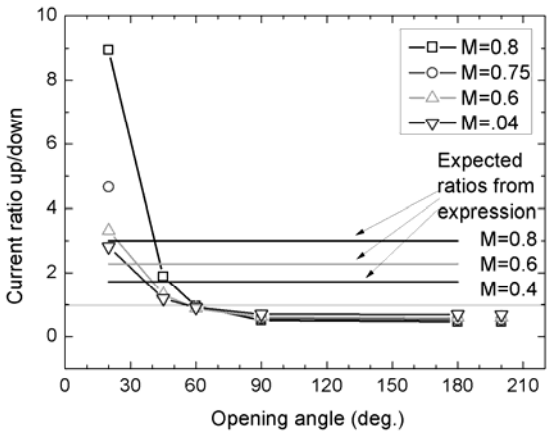

Figure 8. Current ratios computed from the simulated IEDs, as a function of three different subsonic acceptance angles

In Fig. 7 is shown a set of simulated ion energy distributions (IEDs) at 0.6 times the ion acoustic speed c_s, which reach the probe surface through two acceptance angles of 45o and 90o, respectively. On the IEDs observed in the forward direction (facing the source), no effect can be observed from the variation of the acceptance angle. The two distributions overlap almost completely, apart from a very small increase in the low-energy tail of the 90° acceptance angle. With the rearward looking probe, a smaller acceptance angle of 45° leads to a large decrease in the low-energy part of the IED compared to the IED with 90° acceptance angle. This indicates that at the wake side the IED contains a large amount of ions with low energy in the *x* direction. As this low-energy contribution is removed with smaller acceptance angle, it indicates that this part of the distribution has a large y-component, so they

will be ions with a trajectory nearly parallel to the probe surface. They can thus be interpreted as ions originating from the up-stream plasma, with trajectories bent towards the probe and collected at the back side, as reported by others [17, 18, 25].

Ratios representing the up- and downshifted saturation currents were computed from the ratio of the integrated distributions (total counts) between forward and rearward looking probe, according to Eq. 2, for a number of acceptance angles (referred to as opening angle in the plot). The result is shown in Fig. 8 for a set of four different plasma flow speeds, at Mach numbers 0.4, 0.6, 0.8, and a single value of 0.75 at 20^o. The horizontal lines indicate the current ratios as they would be expected from the known speed of the input IED from Eq. 2. It is evident that the larger acceptance angles will yield apparently reversed flows with respect to the true speeds of the IEDs, with a turning point from reversed to forward (ratio=1) flow at an acceptance angle of about 60^o. The turning point is quite independent of the actual flow speed, which indicates that it may depend on the geometry only. However, the sensitivity of the ratio to the acceptance angle is increasing rapidly as the angle is decreasing, and the correct Mach number is derived in a range of the acceptance angle between about 35^o and 32^o. This result imposes a quite severe restriction on the aperture of the RFEA with respect to its distance between the front grid and the collector. In the case of our RFEA, with a 2.0 mm diameter aperture and distance between front grid and collector of 2.4 mm, the acceptance angle is 45^o. We note that the current ratios in the simulated data at 45^o are in the range between 1 and 2, which agrees quite well with the measured ratios of the Fig. 4 b). Thus, we may conclude that a standard analysis of our RFEA data will generally be measuring the right direction of the flow, but will tend to underestimate the speed. On the other hand, the Mach probe, with a much larger acceptance angle of nearly 180^o, will measure reversed flow (ratio < 1), as in the measurements shown in Fig. 4a). It should be noted that the simulations were made for a case of V_p = 45 V, that is, for a situation with a low magnetic field. On the other hand, in our data sets, V_p is in the range between 70-90 V, and hence the data cannot be directly compared. A more extensive study of the effect of magnetic field and plasma potential yet needs to be carried out in order to create a working knowledge about the capabilities of the RFEA as a probe for flow measurements.

5. Conclusions

In this paper, we have explored the feasibility of the Mach probe and the RFEA to be applied to flow measurement in a weakly magnetized, expanding plasma. The analysis of the Mach probe is shown to indicate a flow in the opposite direction to that of the RFEA. The importance of the acceptance angle of the RFEA has been demonstrated with PIC simulation of IEDs for a set of different angles. For plasma potential V_p = 45 V we find that the simulations result in reversed flow at acceptance angles larger than 60^o, and that flows of the correct order would be inferred from the collected IEDs at acceptance angles between 30 to 35 degrees. This result is in good agreement with data from both the Mach and RFEA probes. Further investigations of the role of V_p and magnetization are in process.

References

[1] Charles C and Boswell R W 2004 *Phys. Plasmas* **11** 1706.
[2] Byhring H S, Charles C, Fredriksen A and Boswell R W 2008 *Phys. Plasmas* **15** 102113
[3] Fruchtman A 2006 *Phys. Rev. Lett.* **96** 065002
[4] Lieberman M A, Charles C and Boswell R W 2006 *J. Phys. D* **39** 3294
[5] Meige A, Boswell R W, Charles C and Turner M M 2005 *Phys. Plasmas* **12** 052317
[6] Charles C 2007 Plasma *Sources Sci. Technol.* **16** R1
[7] Lafleur T, Charles C and Boswell R W 2010 *Phys. Plasmas* **17** 043505
[8] Corr C S, Zanger J, Boswell R W and Charles C 2007 *Appl. Phys. Lett.* **91** 241501
[9] Fredriksen A, Mishra L N and Byhring H S 2010 *Plasma Sources Sci. Technol.* **19** 034009
[10] Charles C and Boswell R W 2003 *Appl. Phys. Lett.* **82** 1356
[11] Charles C, Boswell R W and Porteous R K 1992 *J. Vac.Sci. Technol.* A **10** 398

[12] Shikama T, Kado S, Okamoto A, Kajita S and Tanaka S 2005 *Phys. Plasmas* **12** 044504
[13] Hutchinson I H 1988 *Phys. Rev.* A **37** 4358
[14] Hutchinson I H 2003 *Plasma Phys. Contr. Fusion* **45** 1477
[15] Riccardi C, Barni R and Fredriksen A 2004 *Rev. Sci. Instrum.* **75** 4341
[16] Hudis M and Lidsky L M 1970 *J. Appl. Phys.* **41** 5011
[17] Hutchinson I H 2002 *Phys. Plasmas* **9** 1832
[18] Ko E and Hershkowitz N 2006 *Plasma Phys. Contr. Fusion* **48** 621
[19] Charles C 2005 *IEEE Trans. Plasma Sci.* **33** 336
[20] Sun X, Biloiu C, Hardin R and Scime E E 2004 *Plasma Sources Sci. Technol.* **13** 359
[21] Miloch W J 2010 *Plasma Phys. Contr. Fusion in press*
[22] Miloch W J, Kroll M and Block A D 2010 *Phys. Plasmas* **17** 103703
[23] Langdon C K B 1992 *Plasma Physics via Computer Simulation* (Bristol Adam Hilger)
[24] Vahedi V and Surendra M 1995 *Comp. Phys. Comm.* **87** 179
[25] Miloch W J, Gulbrandssen N, Mishra L N \and Fredriksen Å 2010 *Appl. Phys.Lett. in review*